Using an electro-acoustic model of a vented earpiece to predict the ear canal input impedance

Reinhild Roden, Nick Wulbusch, Alexey Chernov, Florian Denk, Matthias Blau

FITTING AN ELECTRO-ACOUSTIC MODEL OF A VENTED EARPIECE TO 3D FEM SIMULATIONS FOR THE PREDICTION OF THE EAR CANAL INPUT IMPEDANCE

Reinhild Roden[1] **Nick Wulbusch**[2] **Alexey Chernov**[2]
Florian Denk[3,4] **Matthias Blau**[1,4]

[1] Institut für Hörtechnik u. Audiologie, Jade Hochschule Oldenburg, Germany
[2] Institut für Mathematik, C. v. Ossietzky Universität Oldenburg, Germany
[3] Medizinische Physik, C. v. Ossietzky Universität Oldenburg, Germany
[4] Cluster of Excellence "Hearing4All"
reinhild.roden@jade-hs.de

ABSTRACT

In order to ensure optimal sound presentation by hearing systems, the sound pressure at the eardrum should be controlled. Since the sound pressure at the eardrum varies individually and direct measurements are tedious, it is desirable to be able to predict it individually, which requires knowledge of the involved transfer functions. For an earpiece with multiple receivers and microphones, an electro-acoustic model was developed in [1]. This model was used to determine the acoustic impedance of the residual ear canal and subsequently to estimate the individual sound pressure at the eardrum. Recently, an improved prototype of the earpiece, featuring an updated design of the vent and arrangement of microphones and receivers, was developed and made available to the public [2]. In this contribution, an electro-acoustic model of the new earpiece is proposed. In addition to modifications of the model structure, the model parameters are now fitted using simulated transfer functions based on a 3D FEM model of the earpiece instead of measurements. This avoids measurement inaccuracies, bypasses the uncertainty of microphone sensitivity and source parameters of the receivers, and offers the advantage of being able to derive impedances at any point of the simulated sound field. Results show that the 1-dimensional electro-acoustic model can be fitted to give very accurate predictions. This in turn promises more accurate results in the subsequent prediction of the sound pressure at the eardrum.

1. INTRODUCTION

Modern hearing systems are expected to fulfill many different functions. They are intended to support pathological and also healthy hearing. They are used for a variety of purposes, e.g. for in-ear monitoring or in environments of augmented reality. This implies numerous simultaneous optimization requirements for signal processing strategies, such as sound pressure equalization, simultaneous feedback canceling, noise suppression and occlusion control. These requirements can be met by the use of several microphones and loudspeakers, effectively creating a multiple input multiple output (MIMO) system.

Figure 1. Photograph of a left and right earpiece (current prototype), with and without dome sealing in the ear canal [2]

In [3] [4], a prototype of an open hearing system was developed with an individual earmold. For this first prototype, electro-acoustic (EA) models of the hearing system and the residual ear canal developed in [1] made it possible to predict the sound pressure at the eardrum from the measured sound pressure in the vent of the hearing system.
Meanwhile a second prototype with a generic shell design and updated transducer placement has been developed and made available to the public [2]. In this contribution an EA model of this second prototype is presented and the optimization of the model parameters is addressed.

2. METHODS

An appropriate EA model structure was designed, corresponding to the geometry of the new vent. Using the method described by [1], the transfer functions between the receivers and microphones and the input impedance of the residual ear canal are obtained from the EA model. These transfer functions and the impedance can be adapted to measurements by fitting the model parameters as proposed in [1]. A methodological contribution of this work is the substitution of the measurements by 3D FEM (Finite Element Method) simulations. The simulation of acoustic fields bypasses measurement uncertainties, initially neglects the influence of receivers and microphones and allows an exact determination of required impedances in the calculated sound field. To this end, 3D FEM models were used to evaluate the transfer functions between receivers and microphones of the hearing system, as described in Section 2.3. In the following, the EA model is fitted to reproduce the transfer functions and the input impedance of the residual ear canal from 3D FEM simulations as accurately as possible (cf. Sec. 2.3). It is shown up to which frequency the acoustics of the vent can be predicted and whether several independent models are advantageous for different frequency ranges. Additionally, a simplification of the EA model is proposed.

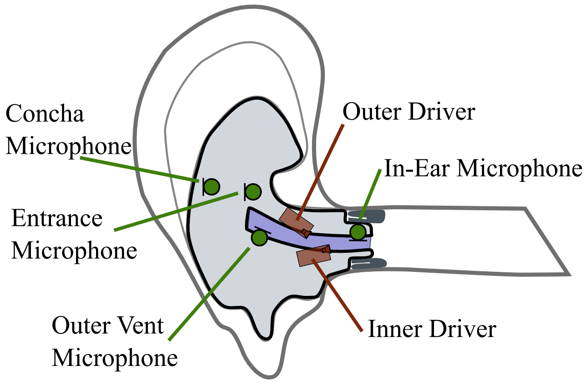

Figure 2. Schematic representation of the current hearing system in the pinna and in the lateral part of the ear canal [2]

2.1 Hearing device

The current prototype of the hearing system [2] has a generic earmold. The vent is more similar to a free straight tube, since microphones and receivers are no longer located in the vent, but are mounted into the walls of the earpiece (cf. Fig. 1, 3). Compared to the earlier prototype, this is expected to result in a nearly planar wave propagation within the duct. A schematic diagram is shown in figure 2.

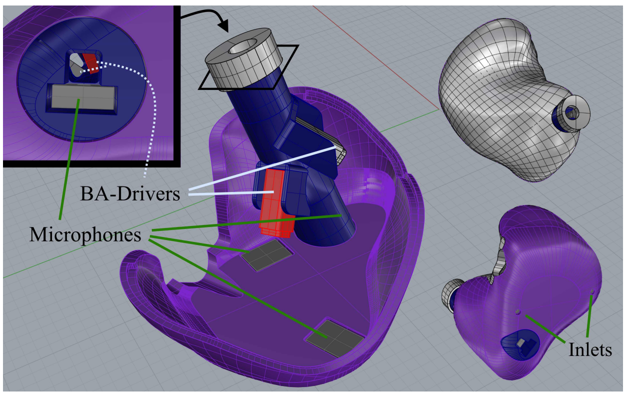

Figure 3. CAD-model of the current hearing system [2]

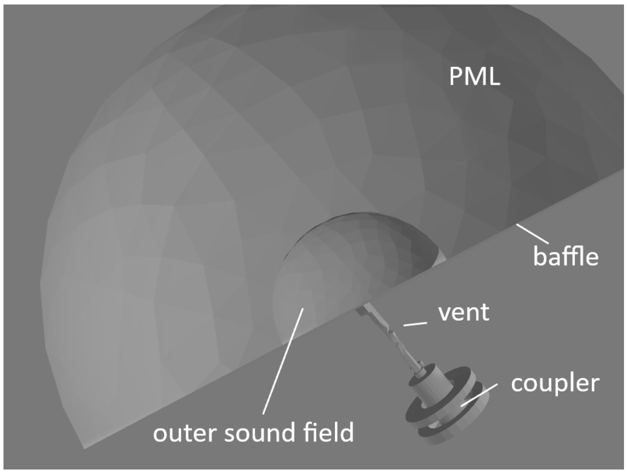

Figure 4. Geometry of the 3D sound field to be simulated. The vent coupled to an IEC711 coupler and the outer sound field (smaller hemisphere, surrounded by the bigger hemisphere (PML)).

2.2 3D FEM Simulation

The software COMSOL Multiphysics 5.4 was used to simulate the internal transfer functions H_{sm} (sources $s = 1, 2$ - inner/outer driver, respectively; mics $m = 1, 2$ - in-ear/outer-vent microphone, respectively). The external sound field to be simulated consisted of a small hemisphere representing the external sound field above an infinite and rigid baffle (cf. Fig. 4). The external sound field is restricted in its extent in order to keep the computational load (which increases with increasing number of the degrees of freedom in the FEM model) feasible even at high frequencies with a finer grid. Free field conditions at the outer boundary were approximated by an absorbing layer (Perfectly Matched Layer, PML). The vent of the earpiece (assumed to be rigid) was coupled to the external sound field in the center of the baffle. Its surface geometry corresponded to the current prototype with built-in microphones and receivers (cf. Fig. 5). An IEC711 coupler was connected to the medial end of the vent. The settings for the FEM simulation of the coupler were taken from the application file provided by COMSOL (Application ID: 12227) [5]. The properties of the coupler can be reproduced very well including thermo-viscous effects and the impedance at the microphone location corresponding to the mechanical properties of a Brüel & Kjær 4192 microphone [6] [7].

Normal velocities $v_{n,rec}$ were applied as excitation onto two sub-areas equal in size S_{rec} (corresponding to the sound outlets of the receivers). The applied surface S_{rec} and the normal velocity $v_{n,rec}$ determine the volume velocity qs,

$$qs = \int v_{n,rec} \mathrm{d}S_{rec} \tag{1}$$

which will be adopted in the later model. Since we were interested in transfer functions only, the value of $v_{n,rec}$ is of no importance, it was chosen arbitrarily and set to 0.001 m/s. The receiving points at which the resulting

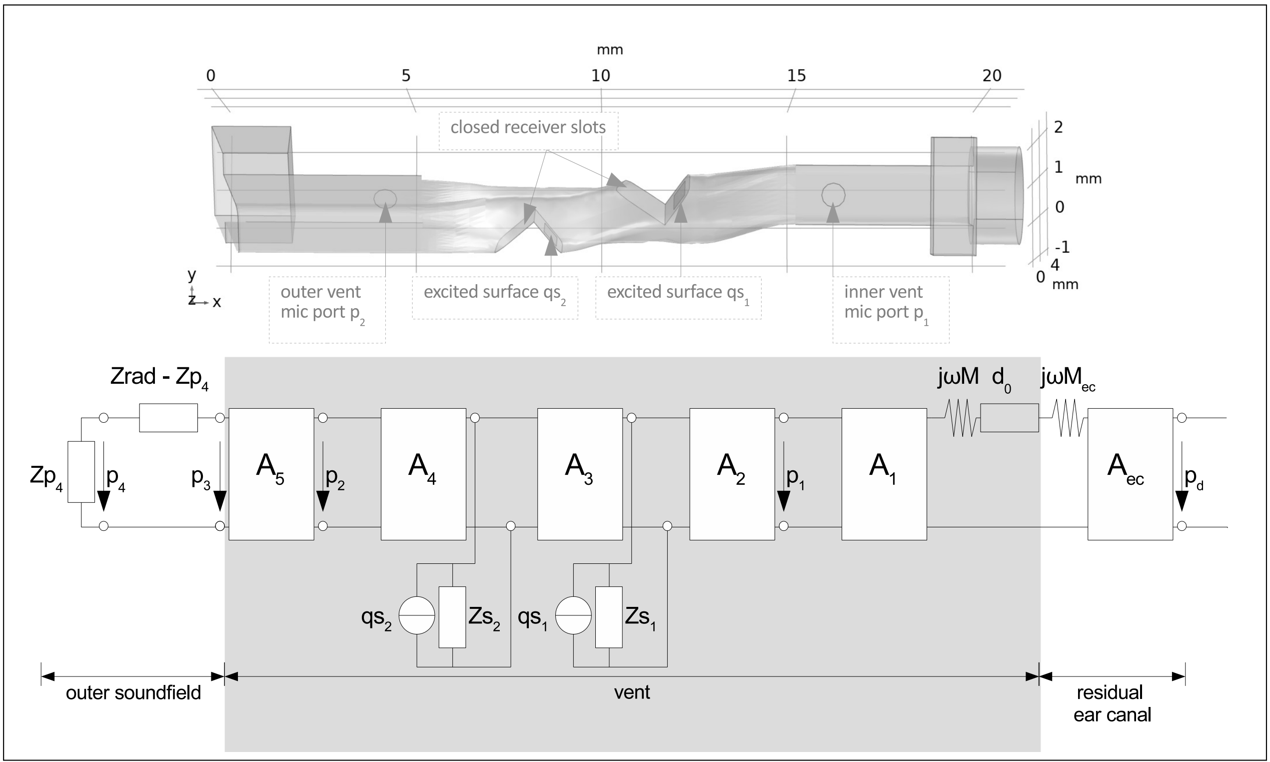

Figure 5. Top: CAD model of the vent equipped with microphones and receivers, Bottom: EA model structure

sound pressure were computed were located at the centers of the microphone ports. The sound pressure was also computed at the coupler microphone and at the points of the entrance and concha microphone (cf. Fig. 1) on the baffle. The transfer functions between drivers and these external microphones were, however, not used to fit the EA model, see Sec. 2.3.

The lateral termination by the radiation impedance Z_{rad} and the transfer impedance Zp_4 was extracted directly from the FEM model (cf. Eq. (2), (3)),

$$Z_{rad} = \frac{\int p \mathrm{d}S_{rad}}{S_{rad} \int v_{n,rad} \mathrm{d}S_{rad}}, \quad (2)$$

$$Zp_4 = \frac{\int p \mathrm{d}S_4}{S_4 \int v_{n,rad} \mathrm{d}S_{rad}}, \quad (3)$$

where p is the complex pressure, $v_{n,rad}$ the normal velocity on the radiating surface S_{rad} and S_4 the surface of the microphone port located in the concha. The input impedance of the residual ear canal Z_{ec} (or in this case that of the coupler) were simulated in a separate 3D FEM model. For this purpose, only the coupler without vent and external sound field was considered and the circular area of the entrance was excited. Results for Z_{ec} correspond very well to values measured in preliminary work [8] [1].

The frequency spectrum of the sound field was simulated at an equidistant frequency resolution of 31.25 Hz up to 16 kHz. This was done in three sub-models for different frequency ranges separated by the frequencies 8 kHz and 12 kHz. The linear frequency distribution was preferred over a logarithmic scale, since resonances in the high frequency range should be resolved with a high resolution. The length of the quadratic finite elements was chosen such that a minimum of six nodes per smallest wavelength for the three frequency ranges was obtained. As a consequence, lower or middle frequencies could be calculated with a smaller number of elements than higher frequencies. Independent of frequency, regions with a high level of geometric detail, such as the vent and the coupler, were meshed with a much finer resolution (in the sub-millimeter range). The numbers of degrees of freedom involved in the 3D FEM simulations for the low, middle and high frequency range were 896602, 1090394 and 1511332, respectively.

2.3 Electro-acoustic model

In the next step, an electroacoustic model is proposed and fitted to the 3D FEM simulations. The general approach follows the preliminary work in [1] [8], except that now simulated transfer functions are used instead of measured ones. The geometry provides an intuitive structure of tube sections, cross-sectional changes, volume velocity sources and coupled impedances, see Fig. 5: the tube-like closed surface of the vent connecting the external sound field to the residual ear canal. The latter is described by the acoustic mass M_{ec} and the two-port A_{ec} including the drum impedance, see the equivalent circuit diagram in Fig. 5. At the output of the equivalent circuit, the sound pressure at the eardrum p_d is obtained. In order to derive the four elements of the two-port A_{ec}, the parameters of the electroacoustic model for the coupler given by [9] were fitted to match the modeled levels with the simulated levels of the input impedance Z_{ec} of the coupler, using the Nelder-

Table 1. Fitted parameters and average absolute level differences in dB of the EA model for five conditions

parameter r_n, l_n [mm]; d_n [1]	initial values	lower constraint	upper constraint	**condition 1** 0.1-8 kHz start values: initial values	**condition 2** 8-14 kHz start values: results of cond. 1	**condition 3** 8-12 kHz start values: results of cond. 1	**condition 4** 0.1-12 kHz start values: results of cond. 1	**condition 5** 0.1-12 kHz start values: results of cond. 1 but d_n=0
r_1	0.8	0	1.60	0.1335	0.2138	0.1256	0.1324	0.1327
l_1	4.00	0	8.00	0	0.0638	0	0	0.0001
d_1	0.1 (0)	0	1.00	0.4355	0	0.5852	0.3307	0
r_2	0.7	0	1.40	0.9041	0.8649	0.9467	0.951	0.9527
l_2	3.00	0	6.00	4.1237	6	4.764	4.5644	4.5852
d_2	0.1 (0)	0	1.00	0	0	0	0	0
r_3	0.8	0	1.60	0.6948	0.1184	0.2889	0.5661	0.5587
l_3	3.8	0	7.60	3.2487	0.0917	0.5295	2.1324	2.0673
d_3	0.1 (0)	0	1.00	0	0.0775	0.0009	0	0
r_4	0.7	0	1.40	0.8143	0.7456	0.8836	0.8365	0.8359
l_4	3.75	0	7.50	4.8796	5.853	5.6178	5.1753	5.1827
d_4	0.1 (0)	0	1.00	0	0	0	0	0
r_5	0.8	0	1.60	0.9324	0.6731	0.6634	0.8836	0.8895
l_5	4.00	0	8.00	4.9549	3.1839	2.6086	4.5326	4.595
d_5	0.1 (0)	0	1.00	0	0	0	0	0
r_0	5.00	0	10.00	3.7929	3.8982	3.6917	3.7818	3.8079
d_0	0.1 (0)	0	1.00	0	0	0	0	0
mean of differences [dB]								
H_{11}				0.1009	1.7438	0.2455	0.1763	0.1744
H_{12}				0.1125	1.0256	0.1881	0.1309	0.1364
H_{21}				0.1379	1.9902	0.2112	0.2724	0.2745
H_{22}				0.1634	2.0261	0.2143	0.2571	0.2581
Z_{ec}				0.0000	0.0097	0.0007	0.0000	0.0001

Mead-Simplex algorithm [10].

In terms of modeling the cross-sectional change at the medial end of the vent, the lossy acoustic mass M with the loss factor d_0 was inserted in series. The two-port A_1 describes the duct section lateral to this cross-sectional change up to the inner microphone ($m = 1$, pressure p_1). The two-ports A_2, A_3, A_4 and A_5 describe acoustic ducts that are located between the sources qs_1 and qs_2 and the microphones $m = 2, 3$ with pressures p_2 and p_3. The two sources include the source impedances Zs_1 and Zs_2, which can be assumed to be infinite and therefore negligible (open circuit voltage). The microphone $m = 3$ (p_3) is located at the outside of the face-plate and close to the vent entrance as shown in Fig. 1. Sound radiation into the external sound field can be modeled by assuming a radiation impedance Z_{rad} that was approximated by a piston in a baffle. This radiation impedance is laterally connected to the two-port A_5. The sound pressure p_4 refers to the location of the concha microphone on the face-plate about 1.4 cm away from the vent entrance. Zp_4 is the transfer impedance between the radiating surface of the vent entrance to the concha microphone.

Plane wave propagation in an acoustic duct of constant radius can be modeled by three parameters (the length of the duct l, its radius r and a loss factor d), cf. e.g. [11] [1]. Using five ducts (given with r_n, l_n, d_n for $n = 1...5$) and the cross-sectional change at the medial end of the vent (given with the radius r_0, and the loss factor d_0) there are 17 parameters to be fitted in the model. In order to represent the volume velocity excitation qs, the normal velocity $v_{n,rec}$ was set to be 0.001 m/s on a surface $S_{rec} = 0.5 \cdot 10^{-6}$ m^2 which equals the values used in the 3D FEM simulation.

For two microphones ($m = 1, 2$) and two receivers ($s = 1, 2$) in the vent there are four transfer functions $H_{sm}(f)$. The input impedance Z_{ec} of the residual ear can be calculated from p_1/qs_1 or from p_1/qs_2 as described in [1] resulting in Z_{model,ec,qs_s} for $s = 1, 2$. The least squares functional $C(p)$ to be minimized in order to fit the electro-acoustic model of the vent defined by its parameters p is given by

$$C(p) = \sum_f \Bigg\{ \sum_{m=1}^{2} \Bigg\{ \sum_{s=1}^{2} \Big\{ (\text{db}(H_{\text{sim},sm}(f)) - \text{db}(H_{\text{model},sm}(f,p)))^2 \Big\} \Bigg\} + \sum_{s=1}^{2} \Big\{ (\text{db}(Z_{\text{sim},ec}(f)) - \text{db}(Z_{\text{model},ec,qs_s}(f,p)))^2 \Big\} \Bigg\}, \tag{4}$$

with the function db(TF)=20·lg(|TF|) [dB] giving the levels of the complex transfer function TF. The cost function $C(p)$ was minimized using the Nelder-Mead-Simplex algorithm [10]. In addition, the model parameters p were subjected to box constraints. The lower constraint enforces positivity of the model parameters. Therefore values of the lower constraint were set to 0. Values of the upper constraint were set to 200% of measured geometric lengths and radii and the maximum for the loss factors was set to the value of 1. During the optimization process it turned out that the values of the upper constraint were not reached and the interval did not have to be increased

(cf. lower and upper constraints in Table 1).
For five conditions outlined below and listed in the five rear columns of Table 1, the EA model was fitted using all simulated frequencies in the frequency range of the condition in question: Condition 1): For a more accurate fitting, the cost function was initially minimized only for the frequency range between 0.1-8 kHz, with geometrically determined initial values for the lengths and radii, and a value of 0.1 for the loss factors. Within the interval given by the lower and upper constraints, initial parameters were randomly generated for 14 additional runs. The parameters corresponding to the run yielding the lowest value of the cost function were then used as initial values for a further run, followed by 14 additional runs. This procedure was repeated once again. Condition 2) supplemented the frequency range with frequencies between 8-14 kHz, starting with the values determined from condition 1). Condition 3) was identical to condition 2), but considered only the frequency range between 8-12 kHz. Condition 4) determined a set of parameters for frequencies between 0.1-12 kHz, starting with values from condition 1). This pre-training for the lower frequencies proved to be useful, since otherwise this range could only be optimized insufficiently, probably caused by the linear frequency scale and the corresponding stronger weighting of higher frequencies in the cost function.
After reviewing the fitted parameters of conditions 1) to 4), a simplification of the model was examined. This simplification consisted in setting all loss factors to zero. More specifically, in condition 5) all loss factors were set to 0 and kept at 0, so that only 11 parameters had to be fitted (cf. Table 1). For condition 5) a pre-training for the frequencies 0.1-8 kHz was performed as described for condition 1), but for constant loss factors.

3. RESULTS AND DISCUSSION

The parameters obtained for the various conditions are shown in Table 1, along with the average absolute level differences [dB] for the inner transfer functions H_{sm} and the input impedance of the attached load (coupler). It turned out that the result of the optimization mostly depends on the start parameters. Figures 6 and 7 show the simulated and modeled levels and the resulting level differences for all conditions, respectively, as a function of frequency. For all conditions except the second, an average accuracy of 1.5 dB was obtained. Considering the average absolute level differences (Table 1), it is concluded that a model can be fitted for the whole frequency range 0.1-12 kHz at once. A "multi-model-approach" with two parameter sets for the lower and higher frequency range (combining condition 1) and 3)) does not result in a much better accuracy. Furthermore, the fitted parameters for the conditions 1) to 4) show a striving of the loss factors towards zero, so that it was to be expected that condition 5) (in which all loss factors were set to zero) resulted in an accurate model as well. This may be due to the boundary conditions in the vent, which were assumed to be rigid, so that possible losses were not

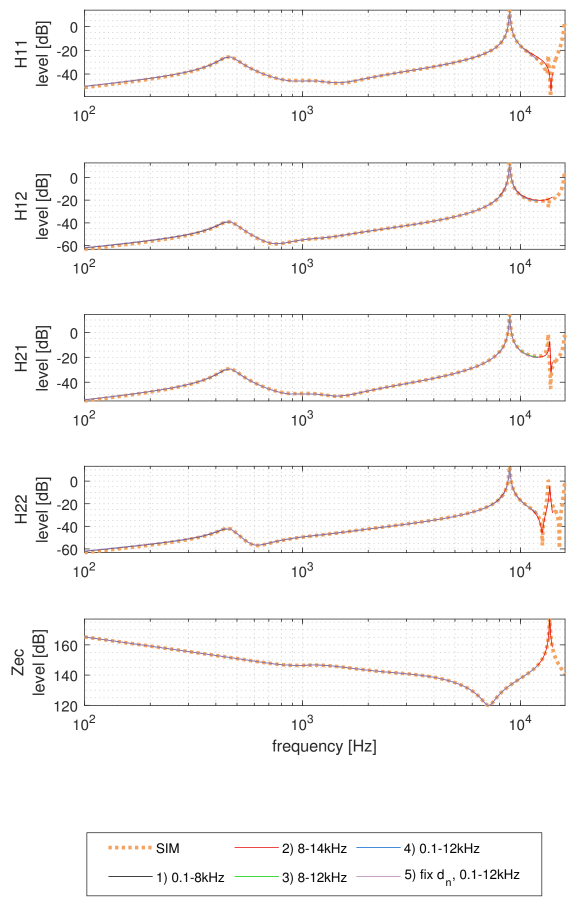

Figure 6. Levels [dB] of simulated and modeled transfer functions

represented in the FEM simulation of the transfer function within the vent. On the other hand, losses were included in the simulation of the attached load (coupler) and in that of the outer sound field, which may already account for most of the total losses.
It is noticeable that fitted "acoustic" lengths and radii can deviate significantly from geometric ones, but the overall length of the vent is well reflected in the resulting parameters.

4. CONCLUSION

For a MIMO hearing system, the acoustics within the vent were simulated using FEM and modeled electro-acoustically. A simplified intuitive structure was found, which allows to represent acoustic transfer functions within the vent as well as the prediction of the acoustic input impedance of an attached IEC711 coupler with high accuracy in the frequency range from 0.1 to 12 kHz, by the use of only 11 parameters.
In future work, we will investigate whether the model is suitable to predict connected impedances of individual residual ear canals. It is expected that additional leakage between the hearing system and the ear canal walls will have to be taken into account.

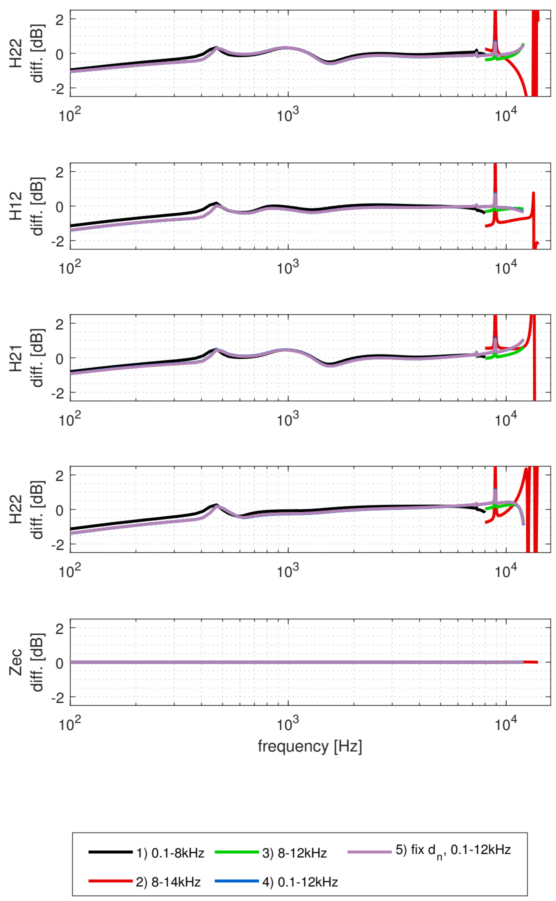

Figure 7. Level differences [dB] between simulated and modeled transfer functions

Funded by the Deutsche Forschungsgemeinschaft (DFG) - Projektnummer 352015383 - SFB 1330 A4 and C1

5. REFERENCES

[1] S. Vogl and M. Blau, “Individualized prediction of the sound pressure at the eardrum for an earpiece with integrated receivers and microphones,” *The Journal of the Acoustical Society of America*, vol. 145, no. 2, pp. 917–930, 2019.

[2] F. Denk, M. Lettau, H. Schepker, S. Doclo, R. Roden, M. Blau, J. Wellmann, and B. Kollmeier, “A one-size-fits-all earpiece with multiple microphones and drivers for hearing device research,” in *Audio Engineering Society Conference: 2019 AES INTERNATIONAL CONFERENCE ON HEADPHONE TECHNOLOGY*, Audio Engineering Society, 2019.

[3] F. Denk, S. Vogl, H. Schepker, B. Kollmeier, M. Blau, and S. Doclo, “The acoustically transparent hearing device: Towards integration of individualized sound equalization, electro-acoustic modeling and feedback cancellation,” in *Proc. 1st International Workshop on Challenges in Hearing Assistive Technology (CHAT-2017)*, pp. 89–94, 2017.

[4] F. Denk, M. Hiipakka, B. Kollmeier, and S. M. Ernst, “An individualised acoustically transparent earpiece for hearing devices,” *International journal of audiology*, vol. 57, pp. 62–70, 2018.

[5] COMSOL, “Generic 711 coupler — an occluded ear-canal simulator.” `https://www.comsol.de/model/download/627341/models.aco.generic_711_coupler.pdf`, [Online; accessed 24-Oct-2020].

[6] Brüel and Kjær, *Microphone Handbook: For the Falcon Range Microphone Products - Technical Documentation*. 1995.

[7] B. L. Zhang, S. Jönsson, A. Schuhmacher, and L. B. Nielsen, “A combined bem/fem acoustic model of an occluded ear simulator,” in *INTER-NOISE and NOISE-CON Congress and Conference Proceedings*, vol. 2004, pp. 260–267, Institute of Noise Control Engineering, 2004.

[8] S. Vogl, T. Sankowsky-Rothe, and M. Blau, “Elektroakustische Modellierung eines Ohrpassstücks mit integrierten Mikrofonen und Lautsprechern,” in *Fortschritte der Akustik (Proceedings of Acoustics)—DAGA*, 2016.

[9] S. Jönsson, B. Liu, L. B. Nielsen, and A. Schuhmacher, “Simulation of couplers,” in *Presentation at the 114th Audio Engineering Society Convention*, pp. 22–25, 2003.

[10] J. A. Nelder and R. Mead, “A simplex method for function minimization,” *The computer journal*, vol. 7, no. 4, pp. 308–313, 1965.

[11] A. H. Benade, “On the propagation of sound waves in a cylindrical conduit,” *The Journal of the Acoustical Society of America*, vol. 44, no. 2, pp. 616–623, 1968.